



# Re-evaluation of the near infrared spectra of mitochondrial cytochrome *c* oxidase: Implications for non invasive in vivo monitoring of tissues



Maria G. Mason, Peter Nicholls, Chris E. Cooper \*

School of Biological Sciences, University of Essex, Wivenhoe Park, Colchester CO4 3SQ, UK

## ARTICLE INFO

### Article history:

Received 10 March 2014

Received in revised form 19 August 2014

Accepted 21 August 2014

Available online 29 August 2014

### Keywords:

Near infrared spectroscopy

NIR

Mitochondria

Cytochrome oxidase

Copper

Cu<sub>A</sub>

## ABSTRACT

We re-determined the near infrared (NIR) spectral signatures (650–980 nm) of the different cytochrome *c* oxidase redox centres, in the process separating them into their component species. We confirm that the primary contributor to the oxidase NIR spectrum between 700 and 980 nm is cupric Cu<sub>A</sub>, which in the beef heart enzyme has a maximum at 835 nm. The 655 nm band characterises the fully oxidised haem *a*<sub>3</sub>/Cu<sub>B</sub> binuclear centre; it is bleached either when one or more electrons are added to the binuclear centre or when the latter is modified by ligands. The resulting 'perturbed' binuclear centre is also characterised by a previously unreported broad 715–920 nm band. The NIR spectra of certain stable liganded species (formate and CO), and the unstable oxygen reaction compounds P and F, are similar, suggesting that the latter may resemble the stable species electronically. Oxidoreduction of haem *a* makes no contribution either to the 835 nm maximum or the 715 nm band. Our results confirm the ability of NIRS to monitor the Cu<sub>A</sub> centre of cytochrome oxidase activity in vivo, although noting some difficulties in precise quantitative interpretations in the presence of perturbations of the haem *a*<sub>3</sub>/Cu<sub>B</sub> binuclear centre.

© 2014 The Authors. Published by Elsevier B.V. This is an open access article under the CC BY license (<http://creativecommons.org/licenses/by/3.0/>).

## 1. Introduction

Mitochondrial cytochrome *c* oxidase is now known to contain four redox active metal centres, two haem and two copper. Historically optical spectroscopy focussed on the strong visible light signals from the haem iron centres, cytochrome *a* [1] and *a*<sub>3</sub> [2]. Any copper was regarded as adventitious [3]. This view changed when electron paramagnetic resonance (EPR) spectroscopy showed detectable copper signals. However, only part of the copper, the 'visible' form (now termed Cu<sub>A</sub>), was detectable; this cupric signal tracked enzyme turnover [4,5] and was linked to parallel near infrared (NIR) optical changes at 830 nm [6].

Chance followed NIR changes in submitochondrial particles but found slow redox behaviour [7]. In contrast, the first detailed kinetic studies by Greenwood and Gibson showed that nearly all the 835 nm component appeared rapidly on pulsing isolated reduced enzyme with oxygen [8,9]. Existence of a second 'invisible' copper centre (now termed Cu<sub>B</sub>), complicated the analysis. Van Gelder claimed one copper centre was responsible for half the NIR absorbance [10,11]. Despite the introduction of techniques for probing EPR invisible copper, such as EXAFS, there remained doubts as to the relative contributions of haems and coppers to the NIR absorbance [12]. However, persuasive evidence for Cu<sub>A</sub> being the dominant NIR chromophore came when it was shown

that strong NIR signals were obtained from isolated protein subunits containing only this chromophore [13]. This view was confirmed when it was shown that homologous bacterial enzymes that lack the Cu<sub>A</sub> centre also lack the corresponding strong NIR absorbance [14].

However, several unresolved questions remain: Cu<sub>B</sub> reduction perturbs the 655 nm band in the oxidised enzyme [15,16]; haem *a* spectral shifts occur upon inhibitory ligand binding to the binuclear centre [17]; the reduced *a*<sub>3</sub>Cu<sub>B</sub> spectrum may include Cu<sub>B</sub>-dependent as well as haem *a*<sub>3</sub> components [18–20]; and other minor NIR absorbance bands are present, generally attributed to ferrous haem *a*<sub>3</sub> [21–23]. Distinguishing different NIR spectral changes is thus essential to analysing oxidase function in vitro.

The NIR 'window' from 680 to 980 nm is also key to monitoring the enzyme in mitochondria, intact cells and whole organisms [24,25] and so to linking enzymatic events with global oxygen metabolism in vivo [26]. Work with intact mammals requires special arrangements to remove the spectroscopic contributions from haemoglobin. Full cytochrome spectroscopy can sometimes be achieved as with bloodless rats, [27,28], but in human beings or other large animals only the NIR 'window' can be used [29].

Discussion has been on-going for a number of years as to whether oxidase activity and control are identical in vitro and in vivo or whether the in vivo system shows unique features. Classical observations in this area were made by Jöbsis [30]. Unique in vivo steady state reduction patterns of cytochromes *a* and *a*<sub>3</sub> were reported for cells and tissues. Current measurements with whole cells have also identified some

Abbreviations: TMPD, N,N,N',N'-Tetramethyl-p-phenylenediamine; NIR, near infrared

\* Corresponding author. Tel.: +44 1206 872752.

E-mail address: [ccooper@essex.ac.uk](mailto:ccooper@essex.ac.uk) (C.E. Cooper).

unusual oxidase species [31]. The possibility of in vivo controls not readily seen in vitro was also emphasized more recently by the observation of labile enzyme phosphorylation in intact systems; unlike enzyme in situ the isolated mammalian enzyme is usually completely dephosphorylated [32].

A range of studies has shown that the NIR spectrum of cytochrome oxidase has potential as a monitor of brain oxygen delivery and/or metabolism [33–36]. Therefore allocating the species contributing to the NIR absorbance changes has clinical as well as basic science relevance. Is the 830 nm signal seen in vivo solely due to cytochrome *c* oxidase cupric Cu<sub>A</sub> or are there other contributors? If the signal is indeed due only to cupric Cu<sub>A</sub> what does it tell us about the overall redox status of the enzyme? Does the redox state of Cu<sub>A</sub> correlate well with oxidase turnover? Our most recent in vitro results [16,37] were interpreted in terms of Cu<sub>A</sub> being always in near equilibrium with the enzyme's redox substrate, cytochrome *c* (although see Hoshi et al. [38] for an alternative view). Therefore as Cu<sub>A</sub> is close to cytochrome *c* in redox potential, and the equilibrium between the two is minimally affected by the energy state of the mitochondrial inner membrane [39], the Cu<sub>A</sub> redox state should reflect that of cytochrome *c*. In turn the latter is believed to provide a measure of oxidase activity.

We have therefore extended our previous analysis [16,37] by examining all the possible NIR signal contributions from cytochrome *c* oxidase, focussing upon the changes in the NIR spectral region at high enzyme concentrations. We conclude, with some caveats, that the 830 nm band is indeed largely due to cupric Cu<sub>A</sub> and that this monitors the enzyme turnover, as previously suggested. The NIR region can also provide information about the oxidase O<sub>2</sub> reaction intermediates.

## 2. Materials and methods

### 2.1. Materials

Beef heart oxidase was prepared as described below. Cytochrome *c* was Sigma type VI (or equivalent) horse heart protein. Beef liver catalase was obtained by diluting Roche Diagnostics catalase 108 810 from beef liver in a slightly alkaline medium. A stock H<sub>2</sub>O<sub>2</sub> sample was prepared from a 30% Sigma-Aldrich aqueous solution. Sodium dithionite, (+)-sodium ascorbate, sodium formate, N,N,N',N'-tetramethyl-*p*-phenylenediamine dihydrochloride (TMPD) lauryl (dodecyl) maltoside, potassium ferricyanide and all buffer salts were analytical reagent or equivalent samples from Sigma-Aldrich. Sodium dithionite solutions (10% w/v) were prepared as required and used within 3 h. CO (carbon monoxide) was 100% BOC compressed gas.

### 2.2. Preparation of cytochrome *c* oxidase

The beef heart enzyme was prepared by the method of Yonetani [18] with minor modifications. Lauryl maltoside was employed as the final

detergent and the detergent extraction was performed at 5 °C. The preparation had an absorbance ratio (280 nm/Soret) of ~2.4 with not more than 5% haem impurity (from analytical HPLC). It was assayed with a turnover number (reducing equivalents per mole cytochrome *aa*<sub>3</sub> per second) of ~250 e<sup>-</sup> s<sup>-1</sup> in the presence of ascorbate/cytochrome *c*/TMPD (10 mM/30 μM/300 μM) at pH 7.4 and at 35 °C.

### 2.3. Preparation of pulsed (fast) form of oxidised enzyme

The resting enzyme (3.6 ml of 75 μM stock cytochrome *aa*<sub>3</sub>), in the presence of a small amount of beef liver catalase, was reduced by the addition of freshly prepared 10% dithionite solution in 0.1 M Na Borate buffer pH 8.75 containing 170 nM catalase. The samples were incubated at room temperature for 15 min and a further 1 h on ice. The enzyme was diluted with buffer (0.1 M Na Borate/0.1% LM, pH 8.75) and then concentrated in a Vivaspin 20 (30,000 MW cut-off filter, Vivascience) by centrifugation (1 h, 1500 g); this process also removes low molecular weight contaminants produced by the treatment. To ensure complete re-oxidation of cytochrome oxidase, potassium ferricyanide aliquots and a further 6 ml buffer were added to the concentrated enzyme sample. Excess ferricyanide was removed by re-centrifugation in the Vivaspin device for a further 40 min. The ferricyanide treatment was repeated (once or twice) until the Soret and visible peak maxima at 423 and 598 nm in the optical spectrum were unchanging at pH 8.75. These pulsed enzyme samples (hereafter referred to as oxidised enzyme) were stored in the pH 8.75 buffer at -80 °C until required.

### 2.4. Spectral acquisition

Data were acquired using Spectrasuite software and a fibre optic system comprising a cooled CCD (QE65000, 25 μm slit width), a tungsten halogen light source (HL-2000-FHSA-HP), 1000 μm optical fibres (QP1000-2-VIS-BX) and either a standard cuvette holder (CUV) (all from Ocean Optics) or a light-integrating sphere with centre mounted cuvette holder (Labsphere, Prolite). Unless otherwise stated the oxidised spectrum was recorded and stored with subsequent spectra acquired as difference spectra relative to oxidised.

### 2.5. Preparation of oxygen intermediates P & F

The P intermediate was obtained by gently blowing CO gas onto the enzyme for 10 s at pH 8.75, with subsequent incubation leading to complete formation after a few minutes. The amount of P formed was calculated using a delta E<sub>M</sub> 607–630 nm = 11,000 M<sup>-1</sup> cm<sup>-1</sup> [40]. The F intermediate was obtained by the addition of peroxide at pH 8.75 (a small aliquot of catalase added during the pulsing procedure was not removed). Upon addition of 5 mM H<sub>2</sub>O<sub>2</sub> a mixture of F & P was formed. The amounts of P and F involved were calculated using simultaneous equations with the extinction coefficients shown in Table 1. Fig. 1

**Table 1**  
Extinction coefficients determined or employed.

Species	pH	Wavelengths(nm)	E(mM <sup>-1</sup> cm <sup>-1</sup> )
O (absolute spectrum)	8.75	423–460	133.3
		598–630	13.75
		825–(750 + 900)/2	0.74
Cu <sub>A</sub> red minus oxidised	7.4	825–(750 + 900)/2	0.60
	8.75	579–630	(5.5)*
F minus O	8.75	606–630	1.05
		436–412	54.3
		606–630	(11.0)*
P minus O	8.75	579–630	2.15
		437–412	49.8
		590–606	9.2
CO reduced minus reduced	8.75	605–630	3.5
Haem <i>a</i> <sub>3</sub> & CuB reduced minus oxidised	8.75	605–630	23.5
Haem <i>a</i> reduced minus oxidised	8.75	605–630	23.5

Determined in this paper apart from: \* Morgan and Wikstrom [40].

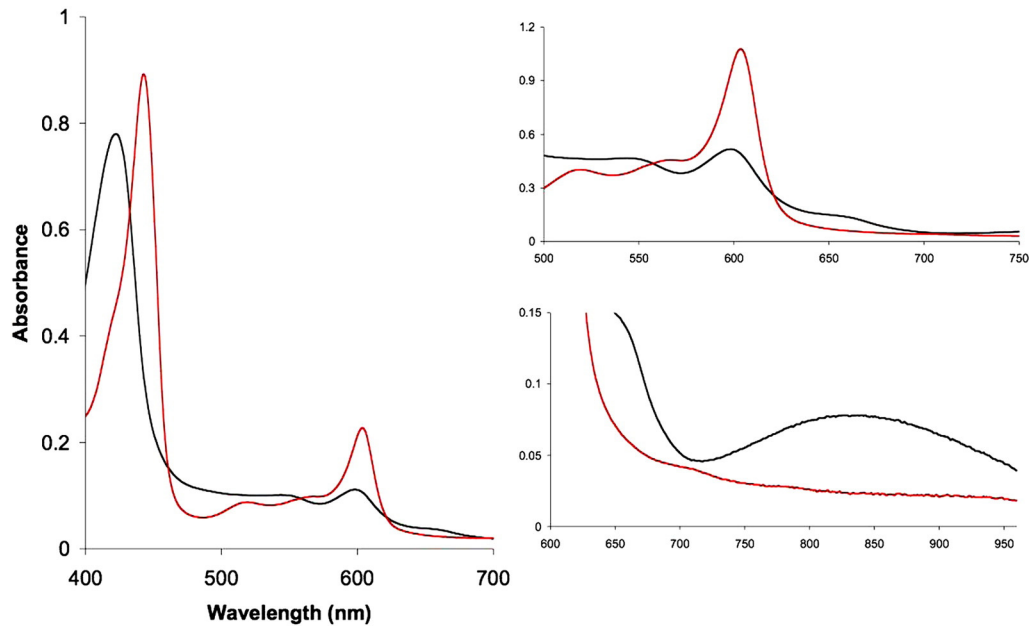


**Fig. 1.** Optical features of oxidised & reduced cytochrome oxidase. Absolute spectra oxidised (black) and fully reduced (red), obtained in the Soret, visible and NIR regions. 0.1 M Na borate buffer pH 8.75 0.1% lauryl maltoside at 22°C. Reduction achieved by addition of a small aliquot of sodium dithionite and acquiring the spectrum shown after 5 min. The main panel shows the spectrum of 4.9 μM enzyme, the inset spectra were acquired at a fivefold higher concentration. The oxidised enzyme spectrum has Soret and visible maxima at 423 nm and 598 nm, respectively. Derived extinction coefficients are shown in Table 1. (For interpretation of the references to color in this figure legend, the reader is referred to the web version of this article.)

shows the absolute spectra of the enzyme (reduced and oxidised) obtained with the QE65000 system (insets show the visible and NIR spectra on expanded scales). The derived extinction coefficients employed are summarised in Table 1. The absolute spectra of pulsed enzyme in the near infrared (NIR) region in both clear and scattering media were also obtained with the integrating sphere technique (results not shown). The spectra were essentially identical with those obtained by conventional spectrophotometry, indicating that none of the broad peaks observed were due to light scattering artefacts.

## 2.6. Spectral deconvolutions

The separated visible and NIR spectra for haem *a*, haem *a*<sub>3</sub> and Cu<sub>A</sub> were calculated via deconvolution of spectra in a variety of redox and ligand states. Table 2 summarises how these were calculated.

## 3. Results

Fig. 2 shows the visible and NIR difference spectra (reduced minus oxidised) of the oxidase obtained in the presence and absence of the

**Table 2**  
Protocols for obtaining cytochrome oxidase difference spectra.

Species measured experimentally	Difference spectra calculated	Resultant species discussed in paper	Location in paper	
I $a^2+a_3^3+$	I – IX	$a^2+a_3^2+ - a^3+a_3^3+$	$a^2+a_3^2+ - a^3+a_3^3+$ (dithionite)	Fig. 2A <sup>a</sup>
	I – III	$a^2+a_3^2+ - a^2+a_3^3+$	$a_3^2+ - a_3^3+$ (dithionite) <sup>a</sup>	a
	I – IV + VIII – IX	$a^2+a_3^2+ - a^3+a_3^3+ + a^3+a_3^3+form - a^2+a_3^3+ form.$	$a_3^2+ - a_3^3+$ (formate)	Fig. 6
	I – II + V – IX	$a^2+a_3^2+ + a^3+a_3^2+ CO - a^2+a_3^2+ CO - a^3+a_3^3+$	$a_3^2+ - a_3^3+$ (CO)	Figs. 2B, 6
II $a^2+a_3^2+ CO$	II – IX	$a^2+a_3^2+ CO - a^3+a_3^3+$	$a^2+a_3^2+ CO - a^3+a_3^3+$	Fig. 2A
	II – I	$a^2+a_3^2+ CO - a^2+a_3^3+$	$a_3^2+ CO - a_3^3+$	Fig. 2B
III $a^2+a_3^3+$	III – IX	$a^2+a_3^3+ - a^3+a_3^3+$	$a^2+ - a^3+$ (dithionite)	a
IV $a^2+a_3^3+$ formate	IV – VIII	$a^2+a_3^3+ form - a^3+a_3^3+ form.$	$a^2+ - a^3+$ (formate)	Fig. 3A
V $a^3+a_3^2+ CO$	V – IX	$a^3+a_3^2+ CO - a^3+a_3^3+$	$a_3^2+ CO - a_3^3+$	Fig. 2B
	II – V	$a^2+a_3^2+ CO - a^3+a_3^3+ CO$	$a^2+ - a^3+$ (CO)	Fig. 2A
VI $a^3+a_3^3+ P$	VI – IX	$a^3+a_3^3+ P - a^3+a_3^3+$	$a_3^3+ P - a_3^3+ c$	Fig. 4B
VII $a^3+a_3^3+ F$	VII – IX	$a^3+a_3^3+ F - a^3+a_3^3+$	$a_3^3+ F - a_3^3+ c$	Fig. 4B
VIII $a^3+a_3^3+$ formate	VIII – IX	$a^3+a_3^3+ form - a^3+a_3^3+$	$a_3^3+ formate - a_3^3+$	b
IX $a^3+a_3^3+$ pulsed				Fig. 1

Deconvoluted difference spectra for cytochromes *a* & *a*<sub>3</sub> using four methods (dithionite kinetics, CO mixed valence spectrum, CN mixed valence spectrum and formate mixed valence spectrum). Note in all cases *a* includes Cu<sub>A</sub> and *a*<sub>3</sub> includes Cu<sub>B</sub>. Reagents in italics e.g. (formate) in column three are used to indicate the different methods by which essentially similar liganded states were calculated. The fourth column indicates where the spectra are illustrated in this paper or where in the literature they were measured.

<sup>a</sup> See Nicholls & Wrigglesworth [20].

<sup>b</sup> See Nicholls [41].

<sup>c</sup> Compounds P and F are detectable only in the fully oxidised state.

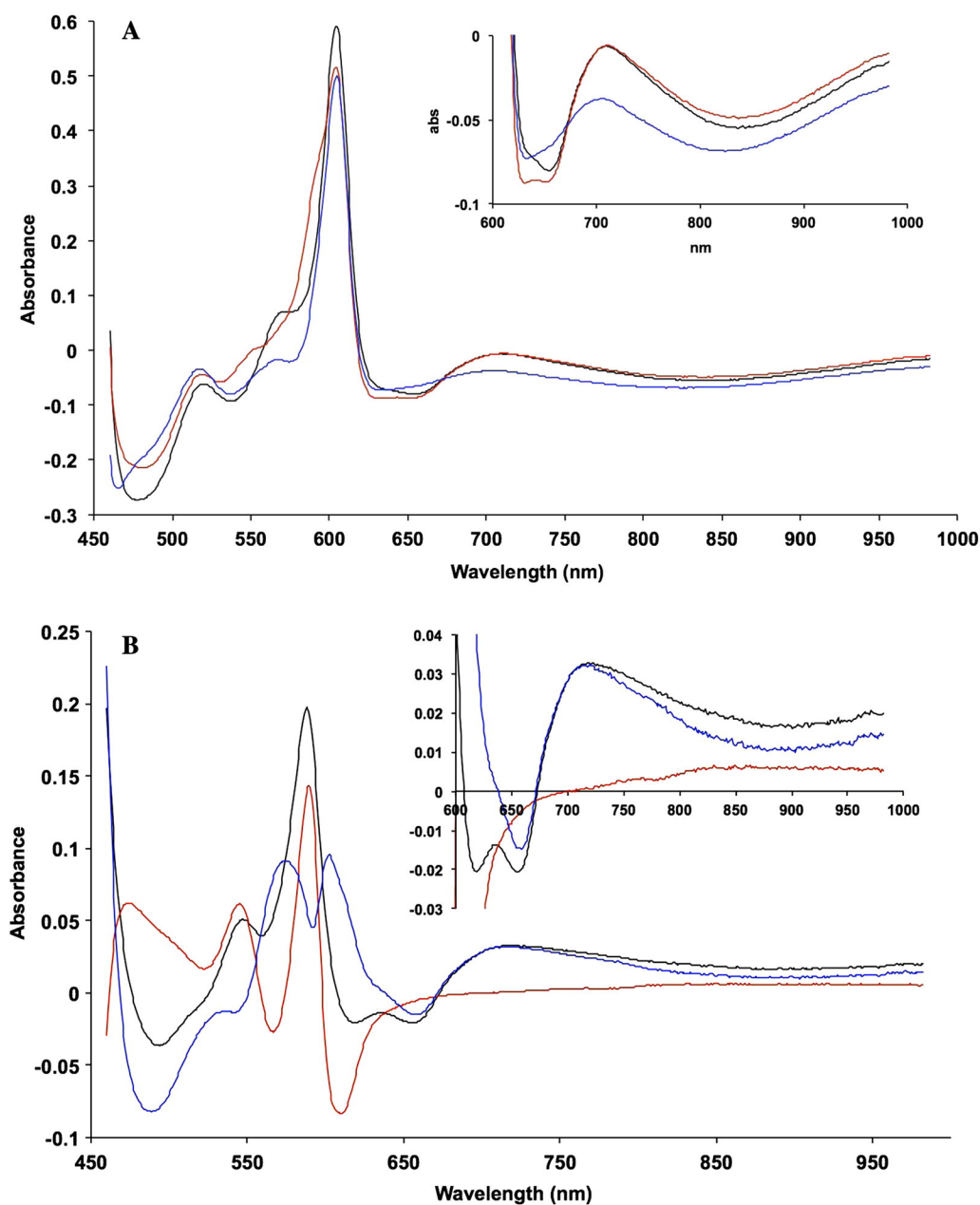


**Fig. 2.** Difference spectra of the reduced, CO-liganded reduced, and mixed valence enzyme. A. Difference spectra plus/minus CO (all with haem *a* and Cu<sub>A</sub> reduced): Reference spectrum was oxidised enzyme in each case (see Fig. 1). Reaction conditions as in Fig. 1. CO complexes (fully reduced and mixed valence) formed as described in Materials and methods (0.1 M Na borate buffer pH 8.75 0.1% lauryl maltoside at 22 °C). ——— fully reduced minus oxidised (I – IX, Table 2); - - - - - fully reduced (plus CO) minus oxidised (II – IX, Table 2); & - - - - - fully reduced (plus CO) minus mixed valence CO (plus ferricyanide, 20 mM) (II – V, Table 2) (i.e. haem *a* & Cu<sub>A</sub> reduced minus oxidised). B. Difference spectra plus/minus CO (all with haem *a* and Cu<sub>A</sub> contributions subtracted): Mixed valence CO complex was prepared as in Materials and methods. Each spectrum represents the calculated difference spectrum of the binuclear centre either in the presence or absence of CO. ——— mixed valence reduced (plus CO) minus oxidised (V – IX, Table 2); - - - - - fully reduced (plus CO) minus fully reduced (unliganded) (II – I, Table 2); & - - - - - mixed valence reduced minus oxidised (fully reduced minus reduced CO plus mixed valence reduced (plus CO) minus oxidised) (I – II + V – IX, Table 2).

binuclear centre ligand CO. In each case the reference spectrum was the oxidised enzyme (as in Fig. 1). Fig. 2A shows three types of difference spectra for the enzyme, in each of which the haem *a* and Cu<sub>A</sub> are both reduced (fully reduced minus oxidised, fully reduced enzyme plus CO minus oxidised and fully reduced CO enzyme minus mixed valence CO enzyme). The inset shows the NIR spectra on an expanded scale. The Cu<sub>A</sub> trough at 835 nm is similar in all three cases but the 655 nm feature (trough) shows characteristic differences. The CO-bound fully reduced enzyme shows a double trough in this region where the unliganded fully reduced enzyme and the third spectrum show only a single trough, albeit in different positions. There is also a trough in the 450–500 nm region with analogous characteristic differences. This is discussed

below. Fig. 2B shows three types of difference spectra, in each of which the haem *a* and the Cu<sub>A</sub> are both oxidised (mixed valence CO minus oxidised, fully reduced CO minus fully reduced, and derived mixed valence reduced minus oxidised). These therefore all provide relevant difference spectra for different states of the binuclear centre. As in Fig. 2A, the inset in Fig. 2B shows the NIR spectra on an expanded scale. The reduced minus oxidised difference spectra, both with and without CO, show a broad feature centred at 710 nm which gives rise to an anomalous apparent trough in the NIR centred near 900 nm (note that Cu<sub>A</sub> is either fully reduced or fully oxidised in each of these spectral pairs). No such feature appears in the reduced CO minus reduced spectrum, whose NIR signature is essentially flat.

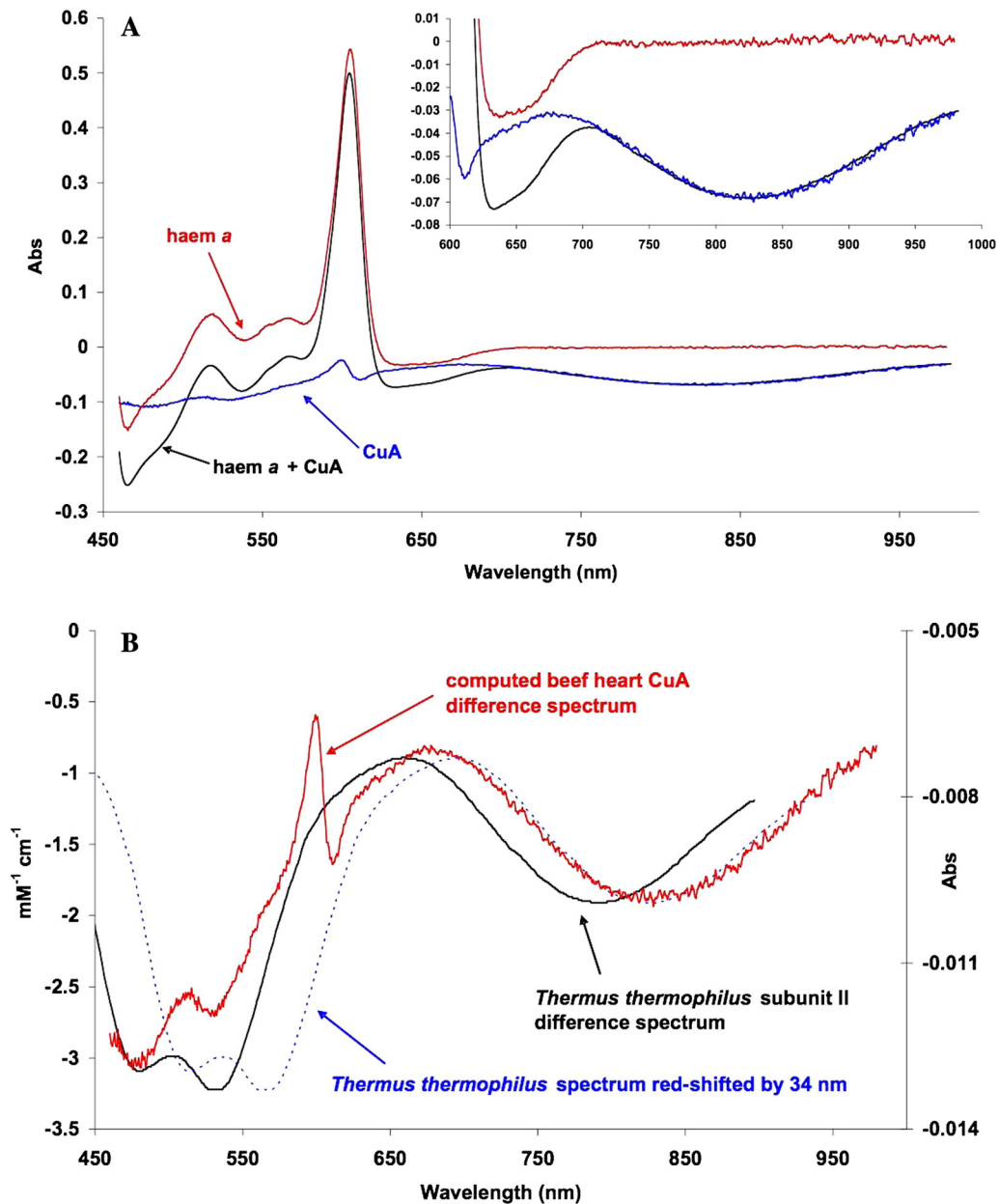


**Fig. 3.** Separated redox difference spectra of cytochrome *a* and  $\text{Cu}_A$ . 0.1 M sodium phosphate buffer pH 7.4 0.1% lauryl maltoside 22 °C. with 7.5 mM sodium formate present in the mixed valence sample (haem *a*  $\text{Cu}_A$  reduced/haem  $a_3$   $\text{Cu}_B$  oxidised). Formate complexes formed as described in **Materials and methods**. A. Separated difference spectra  $\pm$  formate (haem *a* and  $\text{Cu}_A$ ): — formate mixed valence minus oxidised formate (haem *a*  $\text{Fe}^{2+}$  plus  $\text{Cu}_A^+$ ) (IV–VIII, Table 2); - - - formate mixed valence minus calculated  $\text{Cu}_A$  (haem *a*  $\text{Fe}^{2+}$ ); (i.e. haem *a* reduced minus oxidised). - - - - formate mixed valence minus calculated haem *a* ( $\text{Cu}_A^+$ ) (i.e.  $\text{Cu}_A$  reduced minus oxidised). B. Bacterial and mammalian  $\text{Cu}_A$  reduced minus oxidised difference spectra. - - - -  $\text{Cu}_A$  difference spectrum obtained in the presence of formate (converted to extinction coefficients); - - - - *Thermus thermophilus* subunit II difference spectrum (digitised version from the cytochrome oxidase Web site <http://www-bioc.rice.edu/~graham/CcO.Spectra.pc>). The troughs in the visible spectra are closely matched but in the NIR the bacterial subunit II spectrum is blue shifted by ~34 nm relative to the computed cytochrome *c* oxidase  $\text{Cu}_A$ . The 599 to 611 nm spike is due to the haem *a* spectral shift that occurs upon  $\text{Cu}_A$  reduction (see **Discussion**). (For interpretation of the references to color in this figure legend, the reader is referred to the web version of this article.)

**Fig. 3A** shows some analogous spectra for the formate-inhibited system. Here the binuclear centre is held in the fully oxidised state (both haem  $a_3$  and  $\text{Cu}_B$ ) by formate [41]. Slow reduction of the resulting inhibited complex by ascorbate and a low level of TMPD permit a distinction of the  $\text{Cu}_A$  and haem *a* spectra because their redox potentials differ and they remain in thermodynamic equilibrium during the reduction time course. The spectra shown are the combined spectra for the reduction of both components (cf. the corresponding CO-inhibited spectra in **Fig. 2A**) and the deconvoluted spectra for the two separate species, haem *a* alone and  $\text{Cu}_A$  alone. The inset again shows the NIR spectra on an expanded scale. The isolated haem *a* spectrum is featureless in the NIR and contributes nothing to the 835 nm absorbance changes.

Only the spectra with  $\text{Cu}_A$  oxidised minus reduced difference components show an 835 nm band. Conversely only the haem *a* component shows a reduced minus oxidised trough in the 630–650 nm region. However, as well as affecting each other's redox potentials [42], the two centres interact spectrally: the reduced minus oxidised  $\text{Cu}_A$  spectrum shows a blue shift of the alpha (605 nm) peak of haem *a*. That this is a feature of the intact enzyme rather than of the  $\text{Cu}_A$  centre alone is shown by a comparison of the derived  $\text{Cu}_A$  spectrum in **Fig. 3A** with the available spectra of isolated prokaryotic  $\text{Cu}_A$  domains (subunit II species). **Fig. 3B** compares the beef heart  $\text{Cu}_A$  spectrum with that reported for isolated subunit II ( $\text{Cu}_A$ -containing) from *Thermus thermophilus* [43]. The beef heart  $\text{Cu}_A$  835 nm band is red-shifted by 34 nm compared to the prokaryotic spectrum shown here. This red

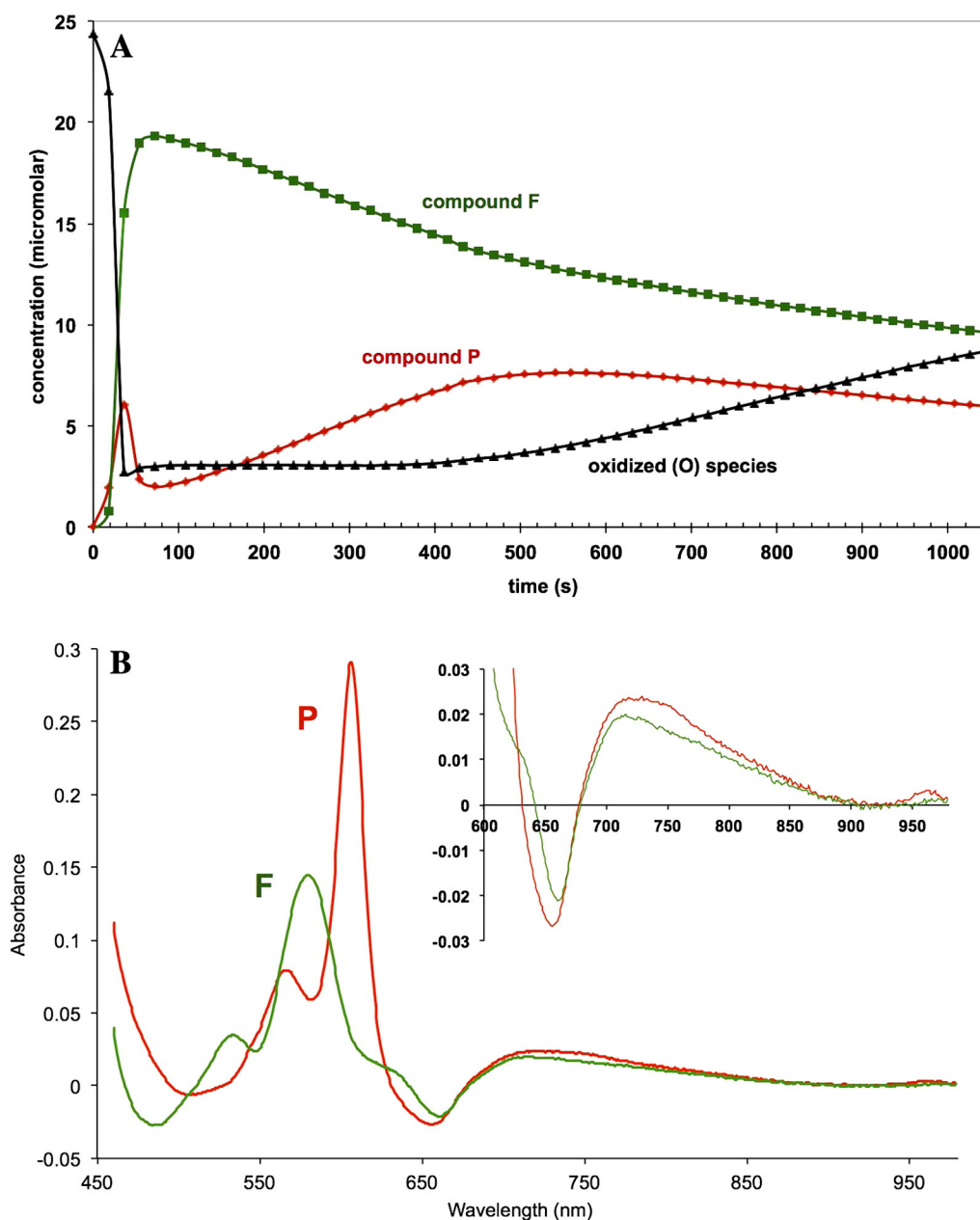


**Fig. 4.** Kinetic and spectral features of the redox intermediates 'P' and 'F'. A. Time course of O, F & P changes after addition of  $\text{H}_2\text{O}_2$  at an alkaline pH,  $24 \mu\text{M}$  cytochrome c oxidase in  $0.1 \text{ M}$  borate buffer pH 8.75  $0.1\%$  lauryl maltoside at  $2^\circ\text{C}$ . Initial oxidation achieved by addition of  $5.2 \text{ mM}$   $\text{H}_2\text{O}_2$  measured at  $10 \text{ s}$ . ——— 'O' (oxidised cytochrome c oxidase); - - - - - 'F' (compound F); - - - - - 'P' (compound P). The green and red traces show the amounts of F and P formed after correcting for the contribution of the other species at the same wavelength pair (as described in *Materials and methods*; cf. *Table 1*). The concentration of 'O' (residual ferric enzyme) is calculated at each time point as  $[\text{O}] = [\text{O}]_{\text{initial}} - ([\text{P}] + [\text{F}])$ . B. Difference spectra of compounds P and F (minus O). pH 8.75; other conditions as in Fig. 4A. - - - - - compound F (VII – IX, *Table 1*); - - - - - compound P (VI – IX, *Table 1*). Difference spectrum of P made by gassing sample with CO (see *Materials and methods*). Difference spectrum of F made from the peroxide-induced spectra (Fig. 4A), corrected for the contribution of species P and total occupancy.

shift of the NIR mammalian centre is also seen relative to the other two prokaryotic spectra in the literature—those of *Paracoccus denitrificans* [44,45] and of *Synechocystis* [46]. The corresponding visible region components (troughs at  $470$  and  $520 \text{ nm}$ ) are located similarly in the eukaryotic and prokaryotic cases. However, only the difference spectrum for intact mammalian enzymes shows the extra feature associated with the haem  $a$   $605 \text{ nm}$  alpha peak, indicating a blue shift in the latter associated with the  $\text{Cu}_A$  reduction.

The NIR characteristics of the enzyme with the binuclear centre in the reduced state, formate-ligated, and CO-ligated, may be compared with the corresponding oxygen intermediates, the so-called 'P' and 'F' states. Fig. 4 illustrates the results obtained. Compound P is obtained from oxidised enzyme by aerobic CO treatment [47] and compound F

by  $\text{H}_2\text{O}_2$  treatment [48]. The CO-induced compound P spectrum (presumed to be compound  $\text{P}_M$ ) is stable over a period of several minutes. The  $\text{H}_2\text{O}_2$ -induced spectra (compound F and some P species) are less stable. Fig. 4A illustrates a time course of peroxide-induced changes. On addition of peroxide to oxidised enzyme in the presence of catalase (to remove excess peroxide within a few seconds) there is immediate formation of an initial compound P species which changes to give largely compound F over a period of tens of seconds. A slow reformation of a second compound P species with the loss of the compound F is then seen over a prolonged period, which terminates with loss of both intermediates and the reformation of oxidised enzyme. The scheme (Fig. 4A & see *Discussion*) summarises the apparent events taking place. Fig. 4B shows the resulting difference spectra of

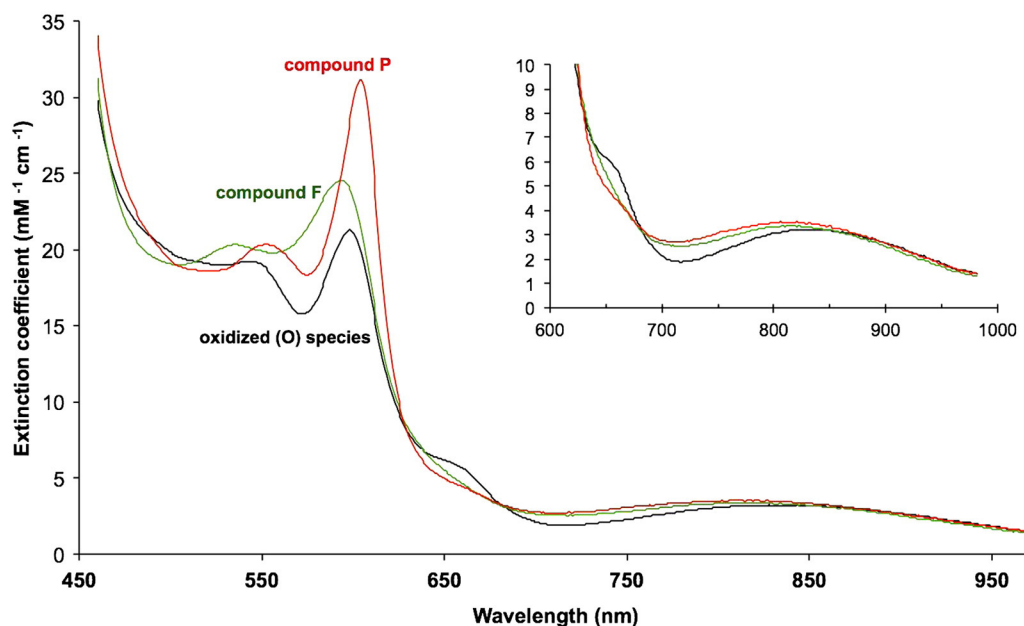


**Fig. 5.** Absolute spectra of O, P, & F. Spectra are plotted in terms of millimolar extinction coefficients (cf. Table 1). — Black = compound O (oxidised state); - - - Red = compound P; - - - Green = compound F. Corrected difference spectra of F minus O and P minus O (Fig. 3B) were normalised to 100% of the starting oxidised spectrum (see Materials and methods; cf. Table 1), and then added to the original absolute oxidised spectrum obtained under the same conditions. pH 8.75, 22°C. (For interpretation of the references to color in this figure legend, the reader is referred to the web version of this article.)

compounds P and F at pH 8.75 (this alkaline pH maximises occupancy of the P state). In addition to the well-known 607 nm alpha peak and 560 nm 'beta' band, compound P shows characteristic features in the NIR region, similar to those seen for the reduced binuclear centre and the reduced-CO bound binuclear centre (Fig. 2B inset) including a trough at 655 nm and a positive feature at 710–720 nm. The difference spectrum of compound F is also shown in Fig. 4C. In addition to the recognised visible region absorbance bands at 540 nm and 580 nm there are again characteristic NIR features, the trough at 655 nm and the broad absorbance centred at 710–720 nm but extending to considerably longer wavelengths (inset).

From the known difference spectra and using these extinction coefficients in Table 1, the absolute spectra of the P and F species can also be obtained. Fig. 5 shows the results and the inset compares the absolute spectra for P, F & O in the NIR region. All three species show the characteristic "835 nm" band but details differ in the 650–800 nm region, because of the existence of two extra characteristic spectral features attributable to the binuclear centre:

- (i) a 660 nm band in the starting oxidised species (O), presumed to be due to the ferric–cupric binuclear centre in the fully oxidised state and absent from both F and P; and,
- (ii) a broad absorbance, centred at 710–720 nm but extending towards the 900 nm region, seen in both P and F forms, which distorts the 835 nm band.

These features are most clearly seen in appropriate difference spectra. Fig. 6 summarises and extends the observations in Fig. 4. This compares not only the P and F spectra but also the putative ferrous  $a_3$ /cuprous CuB spectrum obtained in two ways. The latter can be obtained either by subtracting the haem  $a$ /Cu $_A$  components from a system with the binuclear centre maintained reduced in presence of CO, or by subtracting the haem  $a$ /Cu $_A$  components from a system with the binuclear centre maintained oxidised in presence of formate. Both of these derived spectra and the P & F forms have very similar NIR features involving a 660 nm trough and a 715–920 nm broad peak (compare Figs. 4 and 6).

#### 4. Discussion

This paper describes the first characterisation of both the visible and NIR spectra of mammalian cytochrome oxidase, quantitatively separated into components attributable to haem  $a$ , haem  $a_3$ , Cu $_A$  and the oxygen intermediates P and F. It confirms that the dominant NIR species is the Cu $_A$  centre and its associated redox state changes. However, a new NIR feature has also been characterised that is associated with the binuclear centre. Although broad, this is larger than other absorption bands that have previously been reported in this spectral region. Thus the *Escherichia coli* cytochrome *bo* reduced minus oxidised difference spectrum ([22] has a 758 nm peak ( $\sim 0.25 \text{ mM}^{-1} \text{ cm}^{-1}$ ) which becomes less intense and shifted to 745 nm upon CO addition ( $\sim 0.05 \text{ mM}^{-1} \text{ cm}^{-1}$ ). A similar 784 nm feature is seen with the beef heart enzyme [21]. But these are much smaller than the 715–920 nm feature observed in this paper.

These broad NIR features are common to all the difference spectra involving changes in the binuclear centre, including simple reduction, reduction with ligand (CO) binding, compound P formation and compound F formation. They may thus account for some of the uncertainty concerning the relative contributions of Cu $_A$  and other species to the net NIR changes centred at 835 nm. The latter are purely diagnostic of Cu $_A$  reduction when the binuclear centre is held in a constant redox and ligation state during the changes being monitored. This is most likely the case both aerobically in vitro and during in vivo steady state studies. Under other conditions the situation may prove more complicated.

Use of the 835 nm absorbance must therefore take this possible contribution from the binuclear centre into account. The latter can be held in a constant form either by adding a ligand—cyanide, formate, or carbon monoxide—or by keeping the system fully aerated (which locks the binuclear centre in an oxidised steady state). Changes in the redox state of cytochrome  $a$ , by contrast, do not affect the 835 nm absorbance (Fig. 3A). NIR reduced minus oxidised spectra of cytochrome oxidases from *Bacillus subtilis* membranes also show that the  $aa_3$  quinol oxidase lacking the Cu $_A$  centre has a featureless difference spectrum between 700 and 900 nm, whereas the  $caa_3$  oxidase has a broad NIR feature similar to that of the mitochondrial  $aa_3$  oxidase, except that

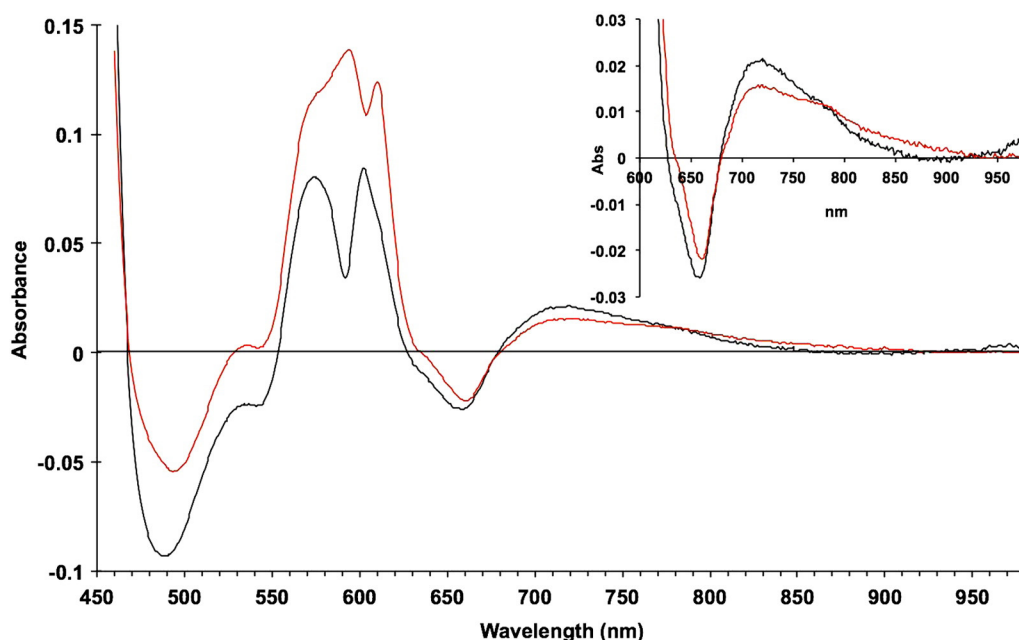


**Fig. 6.** Difference spectra of the cytochrome *c* oxidase binuclear centre in the R and mixed valence R states: modulation of the ferrous spectrum by the redox state of haem *a* and  $\text{Cu}_A$ . ——— Black = reduced haem  $a_3/\text{CuB}$  minus oxidised (from CO fully reduced and mixed valence states, I – II + V – IX, Table 2); conditions as in Fig. 2. - - - - Red = reduced haem  $a_3/\text{CuB}$  minus oxidised (from formate-bound fully oxidised and mixed valence states, I – IV + VIII – IX, Table 2); conditions as in Fig. 3. (For interpretation of the references to color in this figure legend, the reader is referred to the web version of this article.)

the  $\text{caa}_3$  NIR feature has a lower amplitude and is blue-shifted by 40 nm compared to that of mitochondrial oxidase [14].

Some literature discrepancies may be resolvable by attention to these details. For example, by carefully ensuring a constant starting state for the enzyme, we were able to monitor the redox state of  $\text{Cu}_A$  at 835 nm with varying turnover in a kinetically satisfactory way [16]. This contrasted with an earlier study in which initiation of turnover secured an apparent increase in 835 nm absorbance prior to decreases characteristic of reduction [49]. In that case a consistent reduction profile for  $\text{Cu}_A$  could only be achieved in the presence of inhibitors (formate or azide), which lock the binuclear centre into a single spectroscopic state. The initial positive change in the “apparent”  $\text{Cu}_A$  state was almost certainly due to a change at the binuclear centre with a 715–920 nm absorbance increase. As with turnover studies so with redox titrations. Although several groups [50] have obtained classical  $n = 1$

Nernst potentials for the 835 nm component, others showed that the species identified in redox titrations are mixtures in which the 835 nm component may be a minority form [51]. Anaerobic titrations involve continuous redox changes in all the redox-active centres; as several potentials are close in magnitude [16]. As the redox states of any one centre affect both redox potentials and sometimes spectra of the other centres a simple deconvolution becomes impossible.

Spectral interactions between centres are illustrated for haem *a* and  $\text{Cu}_A$  in Fig. 3A & B and for the reduced binuclear centre and haem *a* in Fig. 6. The separated  $\text{Cu}_A$  and haem *a* spectra (Fig. 3B) show an alpha peak shift within the computed  $\text{Cu}_A$  spectrum that must reflect a very small shift in the alpha peak of haem *a* as  $\text{Cu}_A$  is reduced. When the ‘resting’ enzyme is reduced by dithionite the initial (predominantly haem *a* and  $\text{Cu}_A$ ) and final (predominantly haem  $a_3$  and  $\text{CuB}$ ) effects yield by kinetic deconvolution the difference spectra as shown in

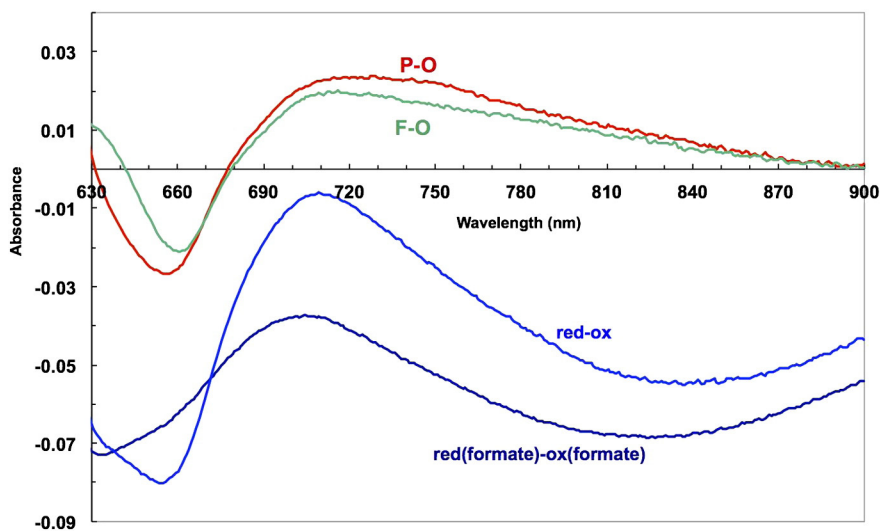


**Fig. 7.** NIR difference spectra of oxidase species with and without  $\text{Cu}_A$  redox features. Data from Figs. 1, 3A and 4B, pH 8.75 & pH 7.4; 24.5  $\mu\text{M}$  cytochrome *c* oxidase; other conditions as in Fig. 4A & B. - - - - compound F minus oxidized (O) (VII – IX, Table 2); pH 8.75. - - - - compound P minus oxidized (O) (VI – IX, Table 2); pH 8.75. - - - - fully reduced minus oxidized (O) (I – IX, Table 2); pH 8.75. - - - - mixed valence (cytochrome  $a^{2+}$ ,  $\text{Cu}_A^+$ ) formate complex minus oxidised formate complex (IV – VIII, Table 2); pH 7.4.



Nicholls & Wrigglesworth [20]. The reduced minus oxidised spectrum of the binuclear centre is characterised by a broad and rather flat-topped absorbance band from 560 to 610 nm. However when obtained by double difference methods (Table 2, Fig. 6) the systems that involve subtraction of a spectrum with haem *a* reduced and the binuclear centre reduced and liganded (CO), or oxidised and liganded (formate), show substantially different spectra in the 600 nm region. The formate system shows a small alpha peak shift, indicating a difference from the pure redox case obtained with dithionite. The carbon monoxide system shows a more substantial shift spectrum in this region. The haem *a* contribution in the 580–610 nm region is very dependent on the redox and ligation state of the binuclear centre. It is therefore all the more surprising to see such close similarities in the NIR region for all these difference spectra (Figs. 4B, 6 and 7). The trough at 655 nm is clearly a reflection of the common changes involved when the ferric-cupric magnetic coupling disappears, both in reduction and in oxidation (to P or F states) of the binuclear centre. But the broad positive absorbance changes in the 715–920 nm region must reflect a change or changes in that centre that are common to the unliganded reduced state (formate data), the CO-bound reduced state, compound P and compound F. We do not currently have a simple model to explain this.

Fig. 7 directly compares the NIR spectra of the various species described in this paper. It illustrates the fact that, even at 100% occupancy, the 715–920 nm feature of the oxygen intermediates P and F does not interfere with methods that directly rely on the spectral shape of the Cu<sub>A</sub> e.g. a three point drop between 790 and 900 nm centred at the 835 nm trough. However, there is the possibility for interference if the complete spectrum is fit over the NIR region and the additional broad absorbing feature is ignored. The NIR absorbance changes of the oxidase have been used for in vivo studies of respiration because the strong NIR signal from the enzyme offsets in part its lower concentration in tissue compared to haemoglobin or myoglobin. However the effects seen in the presence of inhibitors reacting either with the reduced state (e.g. CO) or the oxidised state (e.g. cyanide and formate) show a need for caution in attempting quantitative interpretations.

We conclude that, although the primary contributor to the cytochrome oxidase near infrared spectral signature is cupric Cu<sub>A</sub>, large changes in the population of the oxygen intermediates, P and F, have the potential to confuse the interpretation of in vivo data. Although our in vitro studies on the isolated enzyme suggest that P and F are generally minority populations during steady state turnover [16], there are alternative views [52], most recently from mitochondrial studies [53]. Therefore, although our results confirm the usefulness of NIR to monitor oxidase activity in vivo, we suggest appropriate caution about data interpretation.

## Funding

This work was supported by a grant to CEC from the UK Biotechnology and Biological Sciences Research Council [BB/D017858/1]. The funder played no role in any of: study design; the collection, analysis and interpretation of data; the writing of the report; and the decision to submit the article for publication.

## Acknowledgements

We acknowledge helpful discussions with Professor Mike Wilson (University of Essex).

## References

- [1] D. Keilin, On cytochrome, a respiratory pigment, common to animals, yeast, and higher plants, *Proc. Roy. Soc. B* 98 (1925) 312–339.
- [2] D. Keilin, E.F. Hartree, Cytochrome and cytochrome oxidase, *Proc. Roy. Soc. B* 127 (1939) 167–191.
- [3] A. Ehrenberg, T. Yonetani, Magnetic properties of iron and copper in cytochrome oxidase, *Acta Chem. Scand.* 15 (1961) 1071–1080.
- [4] H. Beinert, D.E. Griffiths, D.C. Wharton, R.H. Sands, Properties of the copper associated with cytochrome oxidase as studied by paramagnetic resonance spectroscopy, *J. Biol. Chem.* 237 (1962) 2337–2346.
- [5] H. Beinert, G. Palmer, Oxidation–reduction of the copper component of cytochrome oxidase. Kinetic studies with a rapid freezing technique, *J. Biol. Chem.* 239 (1964) 1221–1227.
- [6] D.C. Wharton, A. Tzagoloff, Studies on the electron transfer system. LVII. The near infrared absorption band of cytochrome oxidase, *J. Biol. Chem.* 239 (1964) 2036–2040.
- [7] B. Chance, Spectrophotometric observations of absorbance changes in the infrared region in suspensions of mitochondria and in submitochondrial particles, in: J. Peisach, P. Aisen, W.E. Blumberg (Eds.), *The Biochemistry of Copper*, Academic Press, New York & London, 1966, pp. 293–303.
- [8] Q.H. Gibson, C. Greenwood, Kinetic observations on the near infrared band of cytochrome *c* oxidase, *J. Biol. Chem.* 240 (1965) 2694–2698.
- [9] Q.H. Gibson, C. Greenwood, Reactions of cytochrome oxidase with oxygen and carbon monoxide, *Biochem. J.* 86 (1963) 541–554.
- [10] B.F. van Gelder, On cytochrome *c* oxidase. I. The extinction coefficients of cytochrome *a* and cytochrome *a*<sub>3</sub>, *Biochim. Biophys. Acta* 118 (1966) 36–46.
- [11] B.F. van Gelder, A.O. Muijsers, On cytochrome *c* oxidase. II. The ratio of cytochrome *a* to cytochrome *a*<sub>3</sub>, *Biochim. Biophys. Acta* 118 (1966) 47–57.
- [12] L. Powers, W.E. Blumberg, B. Chance, C.H. Barlow, J.S. Leigh Jr., J. Smith, T. Yonetani, S. Vik, J. Peisach, The nature of the copper atoms of cytochrome *c* oxidase as studied by optical and X-ray absorption edge spectroscopy, *Biochim. Biophys. Acta* 546 (1979) 520–538.
- [13] M. Kelly, P. Lappalainen, G. Talbo, T. Haltia, J. van der Oost, M. Saraste, Two cysteines, two histidines, and one methionine are ligands of a binuclear purple copper center, *J. Biol. Chem.* 268 (1993) 16781–16787.
- [14] W. Henning, L. Vo, J. Albanese, B.C. Hill, High-yield purification of cytochrome *aa*<sub>3</sub> and cytochrome *caa*<sub>3</sub> oxidases from *Bacillus subtilis* plasma membranes, *Biochem. J.* 309 (1995) 279–283.
- [15] R. Mitchell, P. Mitchell, P.R. Rich, The assignment of the 655 nm spectral band of cytochrome oxidase, (published erratum appears in *FEBS Lett* 1991 May 6;282(2):449) *FEBS Lett.* 280 (1991) 321–324.
- [16] M.G. Mason, P. Nicholls, C.E. Cooper, The steady-state mechanism of cytochrome *c* oxidase: redox interactions between metal centres, *Biochem. J.* 422 (2009) 237–246.
- [17] P. Nicholls, V. Hildebrandt, Binding of ligands and spectral shifts in cytochrome *c* oxidase, *Biochem. J.* 173 (1978) 65–72.
- [18] T. Yonetani, Studies on cytochrome oxidase I. Absolute and difference absorption spectra, *J. Biol. Chem.* 235 (1960) 845–852.
- [19] W.H. Vanneste, The stoichiometry and absorption spectra of components *a* and *a*-3 in cytochrome *c* oxidase, *Biochemistry* 5 (1966) 838–848.
- [20] P. Nicholls, J.M. Wrigglesworth, Routes of cytochrome *a*<sub>3</sub> reduction. The neoclassical model revisited, *Ann. N. Y. Acad. Sci.* 550 (1988) 59–67.
- [21] P.R. Rich, A.J. Moody, W.J. Ingledeu, Detection of a near infra-red absorption band of ferrohaem *a*<sub>3</sub> in cytochrome *c* oxidase, *FEBS Lett.* 305 (1992) 171–173.
- [22] W.J. Ingledeu, M. Bacon, P.R. Rich, Characterisation of a near infra-red absorption band of the *Escherichia coli* quinol oxidase, cytochrome *o*, which is attributable to the high-spin ferrous haem of the binuclear site, *FEBS Lett.* 305 (1992) 167–170.
- [23] O. Einarsdóttir, K.E. Georgiadis, T.D. Dawes, Evidence for a band III analogue in the near-infrared absorption spectra of cytochrome *c* oxidase, *Biochem. Biophys. Res. Commun.* 184 (1992) 1035–1041.
- [24] F.F. Jobsis, Non-invasive infrared monitoring of cerebral and myocardial oxygen sufficiency and circulatory parameters, *Science* 198 (1977) 1264–1267.
- [25] C.E. Cooper, R. Springett, Measurement of cytochrome oxidase and mitochondrial energetics by near infrared spectroscopy, *Phil. Trans. R. Soc. London B* 352 (1997) 669–676.
- [26] M. Banaji, A. Mallet, C.E. Elwell, P. Nicholls, C.E. Cooper, A model of brain circulation and metabolism: NIRS signal changes during physiological challenges, *PLoS Comput. Biol.* 4 (2008) e1000212.
- [27] M. Ferrari, I. Giannini, A. Carpi, P. Fasella, Non-invasive near infrared spectroscopy of brain in fluorocarbon exchange-transfused rats, *Physiol. Chem. Phys. Med. NMR* 5 (1983) 107–113.
- [28] A.I. Sylvia, C.A. Piantadosi, O<sub>2</sub> dependence of in vivo brain cytochrome redox responses and energy metabolism in bloodless rats, *J. Cereb. Blood Flow Metab.* 8 (1988) 163–172.
- [29] C.E. Elwell, C.E. Cooper, Making light work: illuminating the future of biomedical optics, *Philos. Trans. R. Soc. A Math. Phys. Eng. Sci.* 369 (2011) 4358–4379.
- [30] F.F. Jobsis, Spectrophotometric studies on intact muscle. I. Components of the respiratory chain, *J. Gen. Physiol.* 46 (1963) 905–928.
- [31] N. Kim, M.O. Ripple, R. Springett, Spectral components of the alpha-band of cytochrome oxidase, *Biochim. Biophys. Acta* 1807 (2011) 779–787.
- [32] M. Huttemann, I. Lee, L.I. Grossman, J.W. Doan, T.H. Sanderson, Phosphorylation of mammalian cytochrome *c* and cytochrome *c* oxidase in the regulation of cell destiny: respiration, apoptosis, and human disease, *Adv. Exp. Med. Biol.* 748 (2012) 237–264.
- [33] A.J. du Plessis, J. Newburger, R.A. Jonas, P. Hickey, H. Naruse, M. Tsuji, A. Walsh, G. Walter, D. Wypij, J.J. Volpe, Cerebral oxygen supply and utilization during infant cardiac surgery, *Ann. Neurol.* 37 (1995) 488–497.
- [34] G. Nollert, P. Möhnle, P. Tassan-Prell, I. Uttner, G.D. Borasio, M. Schmoekel, B. Reichart, Postoperative neuropsychological dysfunction and cerebral oxygenation during cardiac surgery, *Thorac. Cardiovasc. Surg.* 43 (1995) 260–264.
- [35] Y. Kakihana, T. Kuniyoshi, S. Isowaki, K. Toba, E. Nagata, N. Okayama, K. Kitahara, T. Moriyama, T. Omae, M. Kawakami, Y. Kanmura, M. Tamura, Relationship between redox behavior of brain cytochrome oxidase and neurological prognosis, *Adv. Exp. Med. Biol.* 530 (2003) 413–419.

- [36] M.M. Tisdall, I. Tachtsidis, T.S. Leung, C.E. Elwell, M. Smith, Increase in cerebral aerobic metabolism by normobaric hyperoxia after traumatic brain injury, *J. Neurosurg.* 109 (2008) 424–432.
- [37] C.E. Cooper, M.A. Sharpe, M.G. Mason, P. Nicholls, Steady state redox levels in cytochrome oxidase: relevance for in vivo near infrared spectroscopy (NIRS), *Adv. Exp. Med. Biol.* 645 (2009) 123–128.
- [38] Y. Hoshi, O. Hazeki, M. Tamura, Oxygen dependence of redox state of copper in cytochrome oxidase in vitro, *J. Appl. Physiol.* 74 (1993) 1622–1627.
- [39] P.R. Rich, I.C. West, P. Mitchell, The location of Cu<sub>A</sub> in mammalian cytochrome c oxidase, *FEBS Lett.* 233 (1988) 25–30.
- [40] M. Wikström, J.E. Morgan, The dioxygen cycle. Spectral, kinetic, and thermodynamic characteristics of ferryl and peroxy intermediates observed by reversal of the cytochrome oxidase reaction, *J. Biol. Chem.* 267 (1992) 10266–10273.
- [41] P. Nicholls, The effect of formate on cytochrome aa3 and on electron transport in the intact respiratory chain, *Biochim. Biophys. Acta* 430 (1976) 13–29.
- [42] A.J. Moody, P.R. Rich, The effect of pH on redox titrations of haem a in cyanide-liganded cytochrome-c oxidase: experimental and modelling studies, *Biochim. Biophys. Acta* 1015 (1990) 205–215.
- [43] C.E. Slutter, D. Sanders, P. Wittung, B.G. Malmstrom, R. Aasa, J.H. Richards, H.B. Gray, J.A. Fee, Water-soluble, recombinant CuA-domain of the cytochrome ba3 subunit II from *Thermus thermophilus*, *Biochemistry* 35 (1996) 3387–3395.
- [44] A. Jasaitis, C. Backgren, J.E. Morgan, A. Puustinen, M.I. Verkhovskiy, M. Wikstrom, Electron and proton transfer in the arginine-54-methionine mutant of cytochrome c oxidase from *Paracoccus denitrificans*, *Biochemistry* 40 (2001) 5269–5274.
- [45] P. Lappalainen, R. Aasa, B.G. Malmstrom, M. Saraste, Soluble CuA-binding domain from the *Paracoccus* cytochrome c oxidase, *J. Biol. Chem.* 268 (1993) 26416–26421.
- [46] M. Paumann, B. Lubura, G. Regelsberger, M. Feichtinger, G. Kollensberger, C. Jakopitsch, P.G. Furtmuller, G.A. Peschek, C. Obinger, Soluble CuA domain of cyanobacterial cytochrome c oxidase, *J. Biol. Chem.* 279 (2004) 10293–10303.
- [47] P. Nicholls, Effects of inhibitory ligands on the aerobic carbon monoxide complex of cytochrome c oxidase, *Biochem. J.* 183 (1979) 519–529.
- [48] J.M. Wrigglesworth, Formation and reduction of a 'peroxy' intermediate of cytochrome c oxidase by hydrogen peroxide, *Biochem. J.* 217 (1984) 715–719.
- [49] P. Nicholls, G.A. Chanady, Titration and steady state behaviour of the 830 nm chromophore in cytochrome c oxidase, *Biochem. J.* 203 (1982) 541–549.
- [50] M. Erecinska, B. Chance, D.F. Wilson, The oxidation-reduction potential of the copper signal in pigeon heart mitochondria, *FEBS Lett.* 16 (1971) 284–286.
- [51] R.W. Hendler, P.A. Harmon, I.W. Levin, Near infrared spectral changes of cytochrome aa3 during potentiometric titrations, *Biophys. J.* 67 (1994) 2493–2500.
- [52] A.J. Moody, Ligation and electronation states of cytochrome-c oxidase in relation to other oxidases and peroxidases, *Biochem. Soc. Trans.* 19 (1991) 617–622.
- [53] D.J. Chess, E. Billings, R. Covian, B. Glancy, S. French, J. Taylor, H. de Bari, E. Murphy, R. S. Balaban, Optical spectroscopy in turbid media using an integrating sphere: mitochondrial chromophore analysis during metabolic transitions, *Anal. Biochem.* 439 (2013) 161–172.